

Helicity form factors for $D_{(s)} \rightarrow A\ell\nu$ process in the light-cone QCD sum rules approach

S. Momeni *

Department of Physics, Isfahan University of Technology, Isfahan 84156-83111, Iran

The helicity form factors of the $D_{(s)} \rightarrow A\ell^+\nu$ with $A = a_1^-, a_1^0, b_1^-, b_1^0, K_1(1270)$ and $K_1(1400)$ are calculated in the light-cone sum rules approach, up to twist-3 distribution amplitudes of the axial vector meson A . In the helicity form factors parametrization the unitarity constraints are applied to the fitting parameters. In addition, the effects of the low-lying resonances are included in series expansions of aforementioned form factors. The properties of the $D_{(s)} \rightarrow A\ell^+\nu$ semileptonic decays are studied by extending the form factors to the whole physical region of q^2 . For a better analysis, a comparison is also made between our results and the predictions obtained using transition form factors via LCSR, 3PSR and CLFQM methods.

I. INTRODUCTION

The weak semileptonic and hadronic decays of charmed mesons, which occur in the presence of strong interaction, are ideal laboratory candidates to determine the quark mixing parameters and the values of the Cabibbo-Kobayashi-Maskawa (CKM) matrix elements and establish new physics beyond the standard model (SM). These meson category masses are (\mathcal{O} 2 GeV), therefore charm decays are helpful to study nonperturbative QCD while, the heavy quark effective theory (HQET) can also be utilized to study D meson decays [1].

$D_{(s)}$ meson decays can be classified into two categories. The first one, which occurs via $c \rightarrow u \ell^+\ell^-$ transition at quark level, is named the flavor changing neutral currents (FCNC) decay. The $D \rightarrow \pi\ell^+\ell^-$, $D \rightarrow \rho\ell^+\ell^-$, $D \rightarrow \pi\gamma$ and $D \rightarrow \rho\gamma$ from the first group, are studied using QCD factorization [2]. The second class, which happens by the semileptonic decay of charm quark $c \rightarrow d(s)\ell\nu$ are analyzed via different approaches. Traditionally, semileptonic decays are explained in terms of transition form factors as a function of the invariant mass of the electron-neutrino pair, q^2 . These form factors which parameterize nonperturbative effects, are measured for $D \rightarrow K\ell\nu$ decay in [3], while, the Light Cone QCD Sum Rule (LCSR) approach is utilized to studying $D \rightarrow \pi(K, \rho)\ell\nu$ decays [4–6]. The form factors of the $D^+ \rightarrow (D^0, \rho^0, \omega, \eta, \eta')\ell^+\nu$ and $D_s^+ \rightarrow (D^0, \phi, K^0, K^{*0}, \eta, \eta')\ell^+\nu$ semileptonic decays have been calculated in the framework of the covariant confined quark model (CCQM) [7, 8]. The semileptonic decays $D \rightarrow (\pi, \rho, K, K^*)\ell\nu$ have been studied using the (HQET) in Ref. [9] and the lattice QCD (LQCD) results for the $D \rightarrow \pi(K, K^*)\ell\nu$ processes are reported in [10–12]. In Ref. [13–19] the semileptonic decays $D_{(s)} \rightarrow f_0(K_0^*)\ell\nu$, $D_{(s)} \rightarrow \pi(K)\ell\nu$, and $D_{(s)} \rightarrow K^*(\rho, \phi)\ell\nu$ have been investigated in the framework of the three-point QCD sum rules (3PSR). The $D \rightarrow a_1, f_1(1285), f_1(1420)$ and $D_{(s)} \rightarrow K_1\ell\nu$ transitions as the $D_{(s)}$ decay to the axial vector mesons, have been calculated by the 3PSR method [20, 21].

In this paper, the helicity form factors for the $D_{(s)}$ decays into axial vectors are calculated with the LCSR. The helicity form factors which can be obtained by contracting the W (or Z) boson polarization vectors and the transition matrix elements, are also functions of q^2 . The relations among the $D_{(s)} \rightarrow A$ transition matrix elements, transition form factors and the helicity ones are presented in Table I.

Matrix element	Transition form factors	Helicity form factors
$\langle A \bar{s}(\bar{d}, \bar{u}) \gamma^\mu \gamma^5 c D_{(s)} \rangle$	A	$\mathcal{H}_{\mathcal{V},0}$
$\langle A \bar{s}(\bar{d}, \bar{u}) \gamma^\mu c D_{(s)} \rangle$	V_0, V_1, V_2	
$\langle A \bar{u} \sigma^{\mu\nu} \gamma^5 q_\nu c D_{(s)} \rangle$	$T_1(q^2)$	$\mathcal{H}_{\mathcal{T},0}$
$\langle A \bar{u} \sigma^{\mu\nu} q_\nu c D_{(s)} \rangle$	$T_2(q^2), T_3(q^2)$	

TABLE I: The $D_{(s)} \rightarrow A$ decay hadronic matrix elements with the corresponding transition and helicity form factors. In this table \mathcal{V} and \mathcal{T} stands for the vector and tensor current, respectively.

There are some advantages in using the helicity form factors:

* e-mail: samira.momeni@ph.iut.ac.ir

- 1) Diagonalizable unitarity relations can be imposed on the coefficients of the helicity form factor parameterization.
- 2) In the helicity form factors, the contributions from the excited states and the spin-parity quantum numbers are considered by relating the dominant poles in the LCSR predictions to low-lying resonances (for more detailed, see [22]).

The masses and quantum numbers J^P of low-lying $D_{(s)}$ resonances with the relations among the helicity form factors are provided in Table II. These masses will be used in the helicity form factors parameterizations. Notice that the mass values for $D_s(1^-)$ and none of the (1^+) states predicted in [23] have been experimentally confirmed yet.

	D meson	Mass(Gev)		D meson	Mass(Gev)
$J^P = 1^-$, $\mathcal{H}_{\nu,1}$	D^+	2.01	$J^P = 1^+$, $\mathcal{H}_{\nu,0}, \mathcal{H}_{\nu,2}$	D^+	2.35
	D^0	2.00		D^0	2.35
	D_s	2.11		D_s	2.46

TABLE II: The masses of low-lying $D_{(s)}$ resonances and their relations to the helicity form factors. The masses are taken from PDG values [24] and the heavy-quark chiral symmetry approach [23].

In [25], the helicity form factors are calculated via LCSR approach for $B \rightarrow \rho$ decay. In this paper, these form factors are evaluated for $D^0 \rightarrow a_1^-(b_1^-)\ell^+\nu$, $D^+ \rightarrow a_1^0(b_1^0)\ell^+\nu$ and $D_{(s)} \rightarrow K_1\ell^+\nu$ decays, which are described by $c \rightarrow d \ell \nu$ transition at quark level. The form factors are also estimated for the $c \rightarrow s \ell \nu$ transition in $D^+ \rightarrow K_1\ell^+\nu$ decay. Here the physical states $K_1 = K_1(1270), K_1(1400)$ are the mixtures of the K_{1A} and K_{1B} in terms of a mixing angle as [26]:

$$\begin{aligned} |K_1(1270)\rangle &= \sin\theta_K |K_{1A}\rangle + \cos\theta_K |K_{1B}\rangle, \\ |K_1(1400)\rangle &= \cos\theta_K |K_{1A}\rangle - \sin\theta_K |K_{1B}\rangle, \end{aligned} \quad (1)$$

where $|K_{1A}\rangle$ and $|K_{1B}\rangle$ are not mass eigenstates. The mixing angle θ_K is determined by various experimental analyses. The result $35^\circ \leq |\theta_K| \leq 55^\circ$ was reported in Ref. [27]. Moreover, two possible solutions were obtained as $|\theta_K| \approx 33^\circ \vee 57^\circ$ in Ref. [28] and as $|\theta_K| \approx 37^\circ \vee 58^\circ$ in Ref. [29]. Using the study of $B \rightarrow K_1(1270)\gamma$ and $\tau \rightarrow K_1(1270)\nu_\tau$ decays, the value of θ_K is estimated as [30]

$$\theta_K = -(34 \pm 13)^\circ. \quad (2)$$

In this study, the branching ratio values are reported for the $D_{(s)} \rightarrow K_1\ell^+\nu$ decays at $\theta_K = -(34 \pm 13)^\circ$.

Our paper is organized as follows: In Sec. II by using the LCSR, the form factors of $D_{(s)} \rightarrow A$ decays are derived. Section. III, is devoted to the numerical analysis of the form factors and the branching ratios for semileptonic and decays. A comparison of our results for the branching ratios with the other approaches and existing experimental data is also made in this section and the last section is reserved for summary.

II. LIGHT CONE QCD SUM RULES FOR $D^0 \rightarrow a_1^-\ell\nu$ HELICITY FORM FACTORS

To calculate the helicity form factors of $D^0 \rightarrow a_1^-\ell\nu$ decay, the following correlation function is considered:

$$\Pi_\sigma^{a_1}(p_i, p_f) = \sqrt{\frac{q^2}{\lambda}} \sum_\alpha \varepsilon_\sigma^{*\mu} \int d^4x e^{iqx} \langle a_1^-(p_f, \varepsilon_\alpha) | \mathcal{T} \{ j_\mu^{int}(x) j_{D^0}^\dagger(0) \} | 0 \rangle, \quad (3)$$

where $p_i, p_f = (p_f^0, 0, 0, |\vec{p}_f|)$ and $q = p_i - p_f$ are the four-momentum of the D^0 , a_1^- and W -boson, respectively. Moreover, $j_\mu^{int} = d\gamma_\mu(1 - \gamma_5)c$ is the interaction current for $D^0 \rightarrow a_1^-$ process and $j_{D^0} = i\bar{u}\gamma_5 c$ is the interpolating current for D^0 meson. In $\Pi_\sigma^{a_1}$ expression, ε_α and ε_σ denote the polarization for a_1 meson and W -boson, respectively as

$$\varepsilon_{\alpha=0} = \frac{1}{m_{a_1^-}}(|\vec{p}_f|, 0, 0, p_f^0), \quad (4)$$

$$\varepsilon_{\alpha=\pm} = \mp \frac{1}{\sqrt{2}}(0, 1, \mp i, 0), \quad (5)$$

$$\varepsilon_{\sigma=0} = \frac{1}{\sqrt{q^2}}(|\vec{q}|, 0, 0, -q^0), \quad (6)$$

with $|\vec{p}_f| = \sqrt{\lambda}/2m_{D^0}$, $p_f^0 = (m_{D^0}^2 + m_{a_1^-}^2 - q^2)/2m_{D^0}$, $|\vec{q}| = |\vec{p}_f|$ and $q^0 = (m_{D^0}^2 - m_{a_1^-}^2 + q^2)/2m_{D^0}$. Also, $\lambda = (t_- - q^2)(t_+ - q^2)$ with $t_{\pm} = (m_{D^0} \pm m_{a_1^-})^2$. Moreover, $\varepsilon_{\sigma=\pm}$ has similar definition as $\varepsilon_{\alpha=\pm}$.

For off-shell W -boson, $\varepsilon_{\sigma=1}$ and $\varepsilon_{\sigma=2}$ are linear combinations of the transverse (\pm) polarization vectors as

$$\varepsilon_{\sigma=1} = \frac{(\varepsilon_{\sigma=-}) - (\varepsilon_{\sigma=+})}{\sqrt{2}} = (0, 1, 0, 0), \quad (7)$$

$$\varepsilon_{\sigma=2} = \frac{(\varepsilon_{\sigma=-}) + (\varepsilon_{\sigma=+})}{\sqrt{2}} = (0, 0, i, 0). \quad (8)$$

In the Light Cone QCD sum rules approach, the correlation function is given in Eq. (3), should be calculated in phenomenological and theoretical representations. Helicity form factors are found to equate both representations of the correlation function through dispersion relation.

The phenomenological side can be obtained by inserting a complete series of the intermediate hadronic states with the same quantum numbers as the interpolating current j_{D^0} . After separating the lowest D^0 meson ground state and applying Fourier transformation, $\Pi_{\sigma}^{a_1}$ is obtained as:

$$\begin{aligned} \Pi_{\sigma}^{a_1} &= \sqrt{\frac{q^2}{\lambda}} \sum_{\alpha} \varepsilon_{\sigma}^{*\mu} \frac{\langle a_1^-(p_f, \varepsilon_{\alpha}) | \bar{d} \gamma_{\mu} (1 - \gamma^5) c | D^0 \rangle \langle D^0 | j_{D^0}^{\dagger}(0) | 0 \rangle}{(m_{D^0}^2 - p_i^2)} \\ &+ \frac{1}{\pi} \sqrt{\frac{q^2}{\lambda}} \sum_{\alpha} \varepsilon_{\sigma}^{*\mu} \int_0^{\infty} \frac{\rho_{\mu}^h(s)}{s - p^2} ds, \end{aligned} \quad (9)$$

where, ρ_{μ} is the density of higher states and continuum which can be approximated using the ansatz of the quark-hadron duality as

$$\rho_{\mu}^h(s) = \rho_{\mu}^{QCD}(s) \theta(s - s_0), \quad (10)$$

where, $\rho_{\mu}^{QCD} = \frac{1}{\pi} \text{Im}(\Pi_{\mu}^{QCD})$ is the perturbative QCD spectral density and s_0 is the continuum threshold in D^0 channel. Now, the following definitions are used for the first and second matrix elements in Eq. (9):

$$\sqrt{\frac{q^2}{\lambda}} \sum_{\alpha} \varepsilon_{\sigma}^{*\mu} \langle a_1^-(p_f, \varepsilon_{\alpha}) | \bar{d} \gamma_{\mu} (1 - \gamma^5) c | D^0 \rangle = \mathcal{H}_{\sigma}^{a_1^-}, \quad \langle D^0 | j_{D^0}^{\dagger}(0) | 0 \rangle = \frac{f_{D^0} m_{D^0}^2}{m_c}, \quad (11)$$

where $\mathcal{H}_{\sigma}^{a_1^-}$, f_{D^0} and m_{D^0} are the helicity form factor of $D^0 \rightarrow a_1^- \ell \nu$ decay, the decay constant and mass of the D^0 meson, respectively. The final result for phenomenological part of correlation function is obtained as:

$$\Pi_{\sigma}^{a_1} = \frac{f_{D^0} m_{D^0}^2}{m_c} \frac{\mathcal{H}_{\sigma}^{a_1^-}}{(m_{D^0}^2 - p_i^2)} + \frac{1}{\pi} \sqrt{\frac{q^2}{\lambda}} \sum_{\alpha} \varepsilon_{\sigma}^{*\mu} \int_0^{\infty} \frac{\rho_{\mu}^h(s)}{s - p^2} ds, \quad (12)$$

To evaluate the correlation function $\Pi_{\sigma}^{a_1}$ in QCD side, the \mathcal{T} product of currents should be expanded near the light cone $x^2 \simeq 0$. After contracting c quark field,

$$\Pi_{\sigma}^{a_1}(p_i, p_f) = -i \sqrt{\frac{q^2}{\lambda}} \sum_{\alpha} \varepsilon_{\sigma}^{*\mu} \int d^4x e^{iqx} \langle a_1^-(p_f, \varepsilon_{\alpha}) | \bar{d}(x) \gamma_{\mu} (1 - \gamma_5) S_c(x, 0) c(0) \rangle | 0 \rangle, \quad (13)$$

is obtained. Where $S_c(x, 0)$ is the full propagator of the c quark. In this paper, the contributions from the gluon contributions have been neglected and only the free propagator is considered as:

$$S_c(x, 0) = \int \frac{d^4l}{(2\pi)^4} e^{-il \cdot x} \frac{\not{l} + m_c}{l^2 - m_c^2} \quad (14)$$

Replacing Eq. (14) in theoretical part of $\Pi_{\sigma}^{a_1}(p_i, p_f)$ yields:

$$\begin{aligned} \Pi_{\sigma}^{a_1}(p_i, p_f) &= -i \sqrt{\frac{q^2}{\lambda}} \sum_{\alpha} \int \frac{d^4l}{(2\pi)^4} \int d^4x \frac{e^{i(q-l)x}}{l^2 - m_c^2} \\ &\times \left\{ \varepsilon_{\sigma}^{*\mu} l^{\nu} \langle a_1^-(p_f, \varepsilon_{\alpha}) | \bar{d}(x) \gamma_{\mu} \gamma_{\nu} \gamma_5 c(0) \rangle | 0 \rangle + \varepsilon_{\sigma}^{*\mu} l^{\nu} \langle a_1^-(p_f, \varepsilon_{\alpha}) | \bar{d}(x) \gamma_{\mu} \gamma_{\nu} c(0) \rangle | 0 \rangle \right. \\ &\left. + m_c \varepsilon_{\sigma}^{*\mu} \langle a_1^-(p_f, \varepsilon_{\alpha}) | \bar{d}(x) \gamma_{\mu} \gamma_5 c(0) \rangle | 0 \rangle - m_c \varepsilon_{\sigma}^{*\mu} \langle a_1^-(p_f, \varepsilon_{\alpha}) | \bar{d}(x) \gamma_{\mu} c(0) \rangle | 0 \rangle \right\}. \end{aligned} \quad (15)$$

As it is clear from Eq. (15), to calculate the theoretical part of the correlation function, the matrix elements of the nonlocal operators between a_1^- meson and vacuum state are needed. Two-particle distribution amplitudes for the axial vector mesons are given in [31], which are put in the Appendix.

In this step, two-particle LCDAs are inserted in Eq. (15), and then integrals over x and l should be evaluated. To estimate these calculations, the following identities are utilized:

$$\gamma_\mu \gamma_\nu = g_{\mu\nu} - i\sigma_{\mu\nu}, \quad (16)$$

$$\gamma_\mu \gamma_\nu \gamma_5 = g_{\mu\nu} \gamma_5 - \frac{1}{2} \varepsilon_{\mu\nu\rho\beta} \sigma^{\rho\beta}, \quad (17)$$

$$\gamma_5 \sigma^{\mu\nu} = -\frac{i}{2} \sigma^{\rho\beta} \varepsilon_{\mu\nu\rho\beta}, \quad (18)$$

$$\epsilon_{\kappa\nu\beta\mu} \epsilon^{\nu\beta\rho\omega} = 2(\delta_\kappa^\rho \delta_\mu^\omega - \delta_\kappa^\omega \delta_\mu^\rho). \quad (19)$$

Now, to get the LCSR calculations for the $D^0 \rightarrow a_1^- \ell \nu$ helicity form factors, the expressions for $\sigma = 0, 1, 2$ from both phenomenological and theoretical sides of the correlation function are equated and Borel transform is applied with respect to variable p_i^2 as:

$$B_{p_i^2}(M^2) \frac{1}{(p_i^2 - m_{D^0}^2)^n} = \frac{(-1)^n}{\Gamma(n)} \frac{e^{-\frac{m_{D^0}^2}{M^2}}}{(M^2)^n}, \quad (20)$$

which eliminates the subtraction term in the dispersion relation and exponentially suppresses the contributions of higher states. Finally, the helicity form factors for $D^0 \rightarrow a_1^- \ell \nu$, transition are obtained in the LCSR as

$$\begin{aligned} \mathcal{H}_0^{a_1^-} = & \frac{m_c f_{a_1^-}}{f_{D^0} m_{D^0}^2} \left\{ -\frac{m_c}{4} \int_{u_0}^1 du \frac{[\Phi_\perp^i(u) - g_\perp^{i,(a)}]}{u^2 M^2} \sqrt{\lambda} e^{\frac{s(u)}{M^2}} + \frac{m_c}{\sqrt{\lambda}} \int_{u_0}^1 du \frac{g_\perp^{i,(a)} \theta_1(q^2)}{u} e^{\frac{s(u)}{M^2}} \right. \\ & + \frac{m_{a_1^-}}{4} \int_{u_0}^1 du \frac{h_\parallel^{(p)}(u) (u+1) \sqrt{\lambda}}{u^2 M^2} e^{\frac{s(u)}{M^2}} + \frac{f_{a_1^-}^\perp}{m_{a_1^-} f_{a_1^-}} \int_{u_0}^1 du \frac{\Phi_\perp(u)}{u} \left[\frac{2 \theta_1(q^2) \theta_2(q^2, u) + \lambda}{\sqrt{\lambda}} \right] e^{\frac{s(u)}{M^2}} \\ & + \frac{4 f_{a_1^-}^\perp m_{a_1^-}}{f_{a_1^-}} \int_{u_0}^1 du \frac{\bar{h}_\parallel^{ii,(t)}(u) \sqrt{\lambda}}{u^2 M^2} \left[1 + \frac{\theta_3(q^2, u) - \theta_2(q^2, u)}{M^2} \right] e^{\frac{s(u)}{M^2}} + \frac{4 f_{a_1^-}^\perp m_{a_1^-}}{f_{a_1^-}} \\ & \times \int_{u_0}^1 du \frac{\bar{h}_\parallel^{ii,(t)}(u)}{u^2} \left[1 - \frac{\theta_2(q^2, u)}{M^2} \right] e^{\frac{s(u)}{M^2}} \Big\}, \end{aligned} \quad (21)$$

$$\begin{aligned} \mathcal{H}_1^{a_1^-} = & -\frac{m_c f_{a_1^-}}{f_{D^0} m_{D^0}^2} \sqrt{\frac{q^2}{2}} \left\{ \frac{m_c m_{a_1^-}}{2} \int_{u_0}^1 du \left[\frac{g_\perp^{(a)}}{u \sqrt{\lambda}} + \frac{g_\perp^{(v)}}{u^2 M^2} \right] e^{\frac{s(u)}{M^2}} - \frac{8 f_{a_1^-}^\perp}{f_{a_1^-}} \int_{u_0}^1 du \frac{\Phi_\perp(u)}{u} e^{\frac{s(u)}{M^2}} \right. \\ & - \frac{32 f_{a_1^-}^\perp m_{a_1^-}^2}{f_{a_1^-}} \int_{u_0}^1 du \frac{\bar{h}_\parallel^{ii,(t)}(u)}{u^2 M^2} e^{\frac{s(u)}{M^2}} - \frac{4 f_{a_1^-}^\perp}{f_{a_1^-}} \int_{u_0}^1 du \frac{\Phi_\perp(u) \theta_2(q^2, u)}{u \sqrt{\lambda}} e^{\frac{s(u)}{M^2}} + \frac{4 f_{a_1^-}^\perp m_{a_1^-}^2}{f_{a_1^-}} \\ & \times \int_{u_0}^1 du \frac{\bar{h}_\parallel^{ii,(t)}(u)}{u^2 \sqrt{\lambda}} \left[1 - \frac{\theta_2(q^2, u)}{M^2} \right] e^{\frac{s(u)}{M^2}} \Big\}, \end{aligned} \quad (22)$$

$$\begin{aligned} \mathcal{H}_2^{a_1^-} = & \frac{m_c f_{a_1^-}}{f_{D^0} m_{D^0}^2} \sqrt{\frac{q^2}{2}} \left\{ \frac{m_c m_{a_1^-}}{2} \int_{u_0}^1 du \left[\frac{g_\perp^{(a)}}{u \sqrt{\lambda}} - \frac{g_\perp^{(v)}}{u^2 M^2} \right] e^{\frac{s(u)}{M^2}} - \frac{8 f_{a_1^-}^\perp}{f_{a_1^-}} \int_{u_0}^1 du \frac{\Phi_\perp(u)}{u} e^{\frac{s(u)}{M^2}} \right. \\ & - \frac{32 f_{a_1^-}^\perp m_{a_1^-}^2}{f_{a_1^-}} \int_{u_0}^1 du \frac{\bar{h}_\parallel^{ii,(t)}(u)}{u^2 M^2} e^{\frac{s(u)}{M^2}} + \frac{4 f_{a_1^-}^\perp}{f_{a_1^-}} \int_{u_0}^1 du \frac{\Phi_\perp(u) \theta_2(q^2, u)}{u \sqrt{\lambda}} e^{\frac{s(u)}{M^2}} - \frac{4 f_{a_1^-}^\perp m_{a_1^-}^2}{f_{a_1^-}} \\ & \times \int_{u_0}^1 du \frac{\bar{h}_\parallel^{ii,(t)}(u)}{u^2 \sqrt{\lambda}} \left[1 - \frac{\theta_2(q^2, u)}{M^2} \right] e^{\frac{s(u)}{M^2}} \Big\}, \end{aligned} \quad (23)$$

where, Φ_\parallel , Φ_\perp are twist-2, $g_\perp^{(a)}$, $g_\perp^{(v)}$, $h_\parallel^{(t)}$ and $h_\parallel^{(p)}$ are twist-3 functions and $\bar{h}_\parallel^{(t)} = h_\parallel^{(t)} - \frac{1}{2} \Phi_\perp(u)$. Moreover, $f_{a_1^-}$ and

$f_{a_1^-}^\perp$ are scale-independent scale-dependent decay constants of the a_1^- meson, respectively [31]. We also have:

$$\begin{aligned}
u_0(s_0) &= \frac{1}{2m_{a_1^-}^2} \left[\sqrt{(s_0 - m_{a_1^-}^2 - q^2)^2 + 4m_{a_1^-}^2(m_c^2 - q^2)} - (s_0 - m_{a_1^-}^2 - q^2) \right], \\
s(u) &= -\frac{1}{u} \left[m_c^2 + u \bar{u} m_{a_1^-}^2 - \bar{u} q^2 - u m_{D^0}^2 \right], \\
\theta_1(q^2) &= \frac{1}{2} (m_{D^0}^2 - m_{a_1^-}^2 - m_{a_1^-}^2 \frac{q^2}{m_{D^0}^2}), \\
\theta_2(q^2, u) &= \frac{1}{u} (3 u^2 m_{a_1^-}^2 + q^2 - m_c^2), \\
\theta_3(q^2, u) &= \frac{1}{u} (-2 u \bar{u} m_{a_1^-}^2 + 2 \bar{u} q^2 - m_c^2), \\
f^{(i)}(u) &\equiv \int_0^u f(v) dv, \quad f^{(ii)}(u) \equiv \int_0^u dv \int_0^v d\omega f(\omega).
\end{aligned} \tag{24}$$

The explicit expressions for twist functions are presented in the Appendix.

Following the previous steps in this section, phrases similar to Eqs. (21, 22, 23) can be obtained for the helicity form factors of $D^0 \rightarrow b_1^- \ell^+ \nu$, $D^+ \rightarrow a_1^0(b_1^0) \ell^+ \nu$, $D^0 \rightarrow K_{1A} \ell^+ \nu$, $D^0 \rightarrow K_{1B} \ell^+ \nu$, $D_s \rightarrow K_{1A} \ell^+ \nu$ as well as $D_s \rightarrow K_{1B} \ell^+ \nu$ decays. For the physical states $K_1(1270)$ and $K_1(1400)$ the following relations are used:

$$\begin{aligned}
\mathcal{H}_\sigma^{K_1(1270)} &= \sin \theta_K \mathcal{H}_\sigma^{K_{1A}} + \cos \theta_K \mathcal{H}_\sigma^{K_{1B}}, \\
\mathcal{H}_\sigma^{K_1(1400)} &= \cos \theta_K \mathcal{H}_\sigma^{K_{1A}} - \sin \theta_K \mathcal{H}_\sigma^{K_{1B}}.
\end{aligned}$$

III. NUMERICAL ANALYSIS

Our numerical analysis for the helicity form factors and branching ratio values of the semileptonic $D_{(s)} \rightarrow A \ell^+ \nu$, are presented in two subsections. The helicity form factors of the semileptonic $D^+ \rightarrow a_1^0(b_1^0, K_{1A}^0, K_{1B}^0) \ell^+ \nu$, $D^0 \rightarrow a_1^-(b_1^-) \ell^+ \nu$, and $D_s^+ \rightarrow K_{1A}^0(K_{1B}^0) \ell^+ \nu$ decays are evaluated in the first subsection. In the second ones, using these form factors, the branching ratio values are estimated for considering decays.

In this work, masses are taken in GeV as $m_c = (1.28 \pm 0.03)$, $m_{D^+(D^0)} = 1.86$, $m_{D_s} = 1.96$, $m_{a_1} = (1.23 \pm 0.40)$, $m_{b_1} = (1.23 \pm 0.32)$ [24], $m_{K_{1A}} = (1.31 \pm 0.06)$ and $m_{K_{1B}} = (1.34 \pm 0.08)$ [31]. The results of the QCD sum rules are used for decay constants of D and D_s and axial vector mesons in MeV, as $f_{D^+(D^0)} = (210 \pm 12)$ and $f_{D_s} = (246 \pm 8)$ [32], $f_{a_1} = (238 \pm 10)$, $f_{b_1} = (180 \pm 8)$, $f_{K_{1A}} = (250 \pm 13)$ and $f_{K_{1B}} = (190 \pm 10)$ [31]. We can take $f_A = f_A^\perp$ at energy scale $\mu = 1$ GeV [31]. The values of Gegenbauer moment for the axial vector mesons, can be found in [31].

A. Analysis of helicity form factors

The formulas of helicity form factors, Eqs. (21, 22, 23), contain two free parameters s_0 and M^2 , which are the continuum threshold and Borel mass-square, respectively. In this paper the values of continuum threshold are chosen as $s_0 = (7 \pm 0.2)$ GeV² [21] and working region for M^2 is provided that the contribution of higher states as well as higher twist contributions, be small.

Fig. 1 shows the dependence of the $D^0 \rightarrow a_1^-$ helicity form factors with respect to M^2 . Since $\mathcal{H}_{\sigma=1,2}$ vanish at $q^2 = 0$, these two form factors are plotted at $q^2 = 0.01$ GeV². It is easily seen from Fig. 1, that the form factors $\mathcal{H}_0^{a_1^-}$, $\mathcal{H}_1^{a_1^-}$ and $\mathcal{H}_2^{a_1^-}$ obtained from the sum rules, can be stable within the Borel parameter intervals $5 \text{ GeV}^2 < M^2 < 8 \text{ GeV}^2$.

The contributions of twist-2 and twist-3 distribution amplitudes and higher states in the $D^0 \rightarrow a_1^-$ helicity form factors, with respect to M^2 , are displaced in Figs. 2 and 3. It can be observed that at the above-mentioned interval from Borel mass, the higher twist contributions as well as higher states, are suppressed. Our numerical analysis shows, that the contribution of the higher states is smaller than about 8% of the total value.

Using all the input values and parameters, the helicity form factors can be evaluated as a function of q^2 . The values of \mathcal{H}_0 for aforementioned decays at the zero transferred momentum square $q^2 = 0$ are presented in Table III. In this table, the contributions of twist-2 distribution amplitudes are also reported. The main uncertainty in $\mathcal{H}_0(q^2 = 0)$ comes from c quark mass m_c and Φ_\perp light cone distribution amplitude.

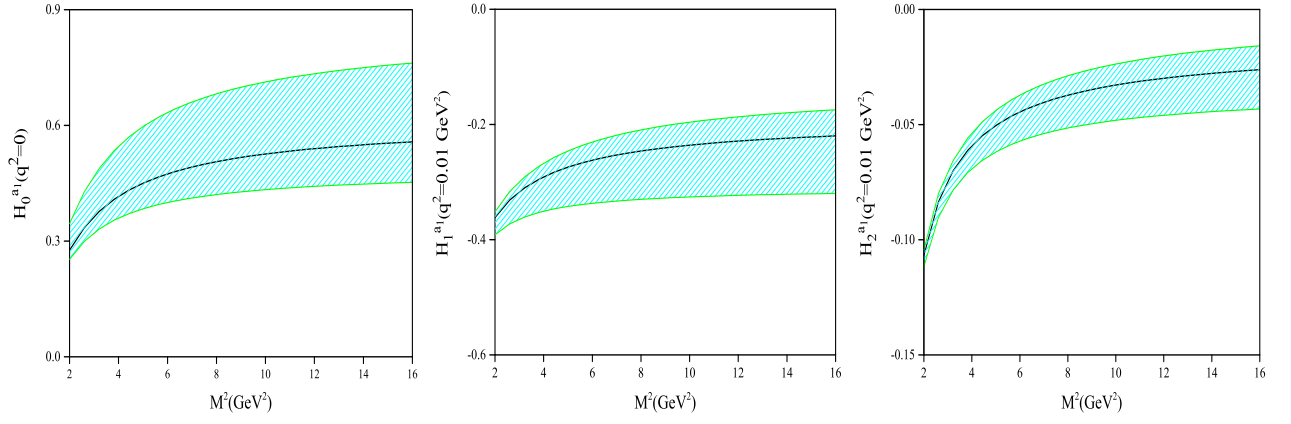


FIG. 1: $D^0 \rightarrow a_1^-$ helicity form factors as functions of M^2 . For $\mathcal{H}_0^{a_1}$ we take $q^2 = 0$ while, for $\mathcal{H}_{1,2}^{a_1}$ the results are plotted at $q^2 = 0.01 \text{ GeV}^2$. The threshold parameter is taken $s_0 = (7 \pm 0.2) \text{ GeV}^2$ for every plot.

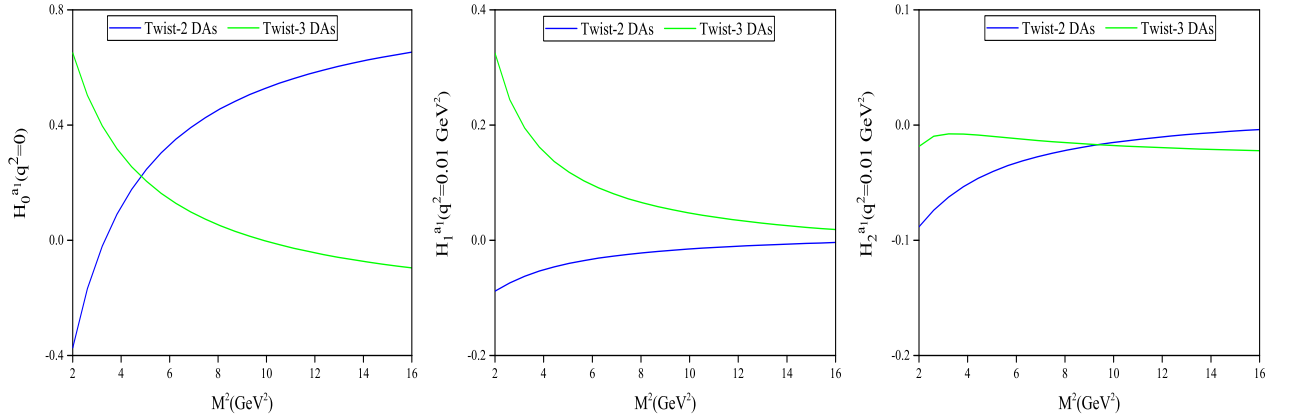


FIG. 2: The contributions of twist-2 and twist-3 distribution amplitudes in the $D^0 \rightarrow a_1^-$ helicity form factors on M^2 and $s_0 = 7 \text{ GeV}^2$. The values of q^2 are taken as Fig. 1.

In order to extend LCSR prediction to the whole physical region, $m_\ell^2 \leq q^2 \leq (m_{D(s)} - m_A)^2$, we use the series

process	$\mathcal{H}_0(q^2=0)$	Twist-2	process	$\mathcal{H}_0(q^2=0)$	Twist-2
$D^0 \rightarrow a_1^- \ell^+ \nu$	$0.67^{+0.26}_{-0.08}$	$0.56^{+0.21}_{-0.05}$	$D^0 \rightarrow b_1^- \ell^+ \nu$	$-0.76^{+0.22}_{-0.19}$	$-0.62^{+0.16}_{-0.10}$
$D^+ \rightarrow a_1^0 \ell^+ \nu$	$0.46^{+0.18}_{-0.05}$	$0.38^{+0.14}_{-0.03}$	$D^+ \rightarrow b_1^0 \ell^+ \nu$	$-0.53^{+0.15}_{-0.13}$	$-0.43^{+0.11}_{-0.10}$
$D \rightarrow K_{1A} \ell^+ \nu$	$0.51^{+0.20}_{-0.04}$	$0.40^{+0.15}_{-0.03}$	$D \rightarrow K_{1B} \ell^+ \nu$	$-0.95^{+0.25}_{-0.21}$	$-0.83^{+0.21}_{-0.15}$
$D_s \rightarrow K_{1A} \ell^+ \nu$	$0.31^{+0.14}_{-0.12}$	$0.21^{+0.11}_{-0.08}$	$D_s \rightarrow K_{1B} \ell^+ \nu$	$-0.40^{+0.15}_{-0.18}$	$-0.32^{+0.11}_{-0.12}$

TABLE III: Helicity form factor \mathcal{H}_0 as well as contribution of twist-2 distribution amplitudes of the $D^+ \rightarrow a_1^0(b_1^0) \ell^+ \nu$, $D^0 \rightarrow a_1^-(b_1^-) \ell^+ \nu$, $D \rightarrow K_{1A}(K_{1B}) \ell^+ \nu$ and $D_s \rightarrow K_{1A}(K_{1B}) \ell^+ \nu$ decays at $q^2 = 0$.

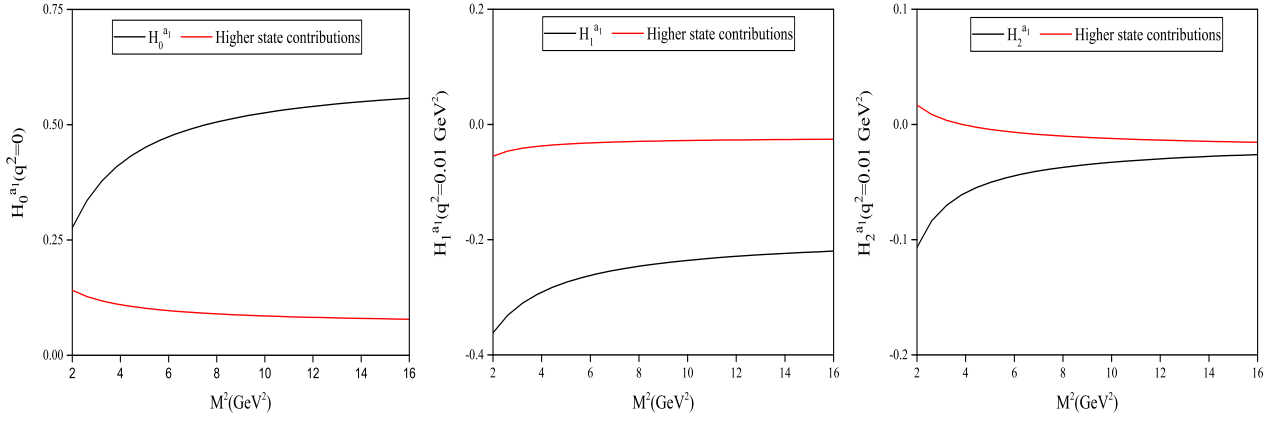


FIG. 3: $D^0 \rightarrow a_1^-$ helicity form factors as a function of M^2 for $s_0 = 7 \text{ GeV}^2$ as well as the higher states contributions in these form factors. The values of q^2 are chosen as Fig. 1.

expansion given in [22] as:

$$\mathcal{H}_0^A(q^2) = \frac{1}{z(q^2, m_{D(s)}^2) \sqrt{z(q^2, t_-)} \phi(q^2)} \sum_{k=0,1} a_k^{A,0} z^k(q^2, t_0), \quad (25)$$

$$\mathcal{H}_1^A(q^2) = \frac{\sqrt{-z(q^2, 0)}}{z(q^2, m_{D(s)}^2) \phi(q^2)} \sum_{k=0,1} a_k^{A,1} z^k(q^2, t_0), \quad (26)$$

$$\mathcal{H}_2^A(q^2) = \frac{\sqrt{-z(q^2, 0)}}{z(q^2, m_{D(s)}^2) \sqrt{z(q^2, t_-)} \phi(q^2)} \sum_{k=0,1} a_k^{A,2} z^k(q^2, t_0), \quad (27)$$

where

$$z(q^2, t) = \frac{\sqrt{t_+ - q^2} - \sqrt{t_+ - t}}{\sqrt{t_+ - q^2} + \sqrt{t_+ - t}}, \quad (28)$$

$$\sqrt{-z(q^2, 0)} = \sqrt{q^2}/m_{D(s)}, \quad (29)$$

where $t = t_0, t_-, m_{D(s)}$ with $t_{\pm} = (m_{D(s)} \pm m_A)^2$ and $t_0 = t_+(1 - \sqrt{1 - t_-/t_+})$. Moreover, $D_{(s)}^r$ shows the resonance states are given in Table II. The function $\phi(q^2)$ is given by [33]:

$$\phi(q^2) = \sqrt{\frac{3t_+t_-}{32\pi\chi_0}} \left(\frac{z(q^2, 0)}{-q^2} \right)^2 \left(\frac{z(q^2, t_0)}{t_0 - q^2} \right)^{-0.5} \left(\frac{z(q^2, t_-)}{t_- - q^2} \right)^{-0.25} \left(\frac{(t_+ - q^2)^2}{t_+ - t_0} \right)^{0.25}, \quad (30)$$

where χ_0 has been calculated using OPE and is given by [22]:

$$\chi_0 = \frac{1 + 0.751\alpha_s(m_c)}{8\pi^2} \quad (31)$$

It should be noted that for the functions $\sqrt{z(q^2, t_-)}$ and $\phi(q^2)$ the replacement $m_{D(s)} \rightarrow m_{D(s)}^r$ must be made. For the series expansion parameterizations 25, 26 and 27, the unitarity constraints are obtained as [22]:

$$\sum_{k=0,1} \left\{ (a_k^{A,0})^2 + (a_k^{A,1})^2 + (a_k^{A,2})^2 \right\} \leq 1 \quad (32)$$

We use parameter Δ defined as:

$$\Delta = \frac{\sum_{q^2} |\mathcal{H}_\sigma^A(q^2) - \mathcal{H}_\sigma^{A,\text{fit}}(q^2)|}{\sum_{q^2} |\mathcal{H}_\sigma^A(q^2)|} \times 100, \quad (33)$$

where $0 \leq q^2 \leq (m_{D(s)} - m_A)^2/2$ to estimate quality of fit for each helicity form factor. Table IV includes the values of a_1^r , a_2^r and Δ for the helicity form factors of the semileptonic decays. For these results all the input parameters are

TABLE IV: Values of b_0 , b_1 and b_2 related to $F^{(1)}(q^2)$ for the fitted form factors of $D_{(s)} \rightarrow a_1, b_1, K_{1A}$ and K_{1B} transitions.

Form factor	a_1	a_2	Δ	Form factor	a_1	a_2	Δ
$\mathcal{H}_0^{D^0 \rightarrow a_1^-}$	0.05	-0.95	0.36	$\mathcal{H}_0^{D^0 \rightarrow b_1^-}$	-0.10	0.49	0.32
$\mathcal{H}_1^{D^0 \rightarrow a_1^-}$	-0.07	-0.56	0.26	$\mathcal{H}_1^{D^0 \rightarrow b_1^-}$	0.12	-0.54	0.17
$\mathcal{H}_2^{D^0 \rightarrow a_1^-}$	-0.12	0.83	0.24	$\mathcal{H}_2^{D^0 \rightarrow b_1^-}$	0.10	-0.87	0.50
$\mathcal{H}_0^{D^+ \rightarrow a_1^0}$	0.03	-0.67	0.35	$\mathcal{H}_0^{D^+ \rightarrow b_1^0}$	-0.07	0.34	0.31
$\mathcal{H}_1^{D^+ \rightarrow a_1^0}$	-0.04	-0.39	0.26	$\mathcal{H}_1^{D^+ \rightarrow b_1^0}$	0.08	-0.38	0.16
$\mathcal{H}_2^{D^+ \rightarrow a_1^0}$	-0.09	0.59	0.24	$\mathcal{H}_2^{D^+ \rightarrow b_1^0}$	0.07	-0.61	0.48
$\mathcal{H}_0^{D \rightarrow K_{1A}}$	0.12	-0.54	0.57	$\mathcal{H}_0^{D \rightarrow K_{1B}}$	-0.04	0.68	0.83
$\mathcal{H}_1^{D \rightarrow K_{1A}}$	-0.09	-0.85	0.30	$\mathcal{H}_1^{D \rightarrow K_{1B}}$	0.16	-0.71	0.57
$\mathcal{H}_2^{D \rightarrow K_{1A}}$	-0.02	0.08	0.29	$\mathcal{H}_2^{D \rightarrow K_{1B}}$	0.16	-0.90	0.54
$\mathcal{H}_0^{D_s \rightarrow K_{1A}}$	0.02	0.85	0.17	$\mathcal{H}_0^{D_s \rightarrow K_{1B}}$	-0.05	0.72	0.22
$\mathcal{H}_1^{D_s \rightarrow K_{1A}}$	-0.07	-0.76	0.05	$\mathcal{H}_1^{D_s \rightarrow K_{1B}}$	0.12	-0.82	0.19
$\mathcal{H}_2^{D_s \rightarrow K_{1A}}$	-0.01	-0.14	0.05	$\mathcal{H}_2^{D_s \rightarrow K_{1B}}$	0.04	-0.77	0.11

set to be their central values. As it can be seen from the values of Δ parameters, are reported in IV, the fit functions 25, 26 and 27 cover the LCSR predictions for the helicity form factors.

The dependence of the form factors \mathcal{H}_0 , \mathcal{H}_1 and \mathcal{H}_2 for $D^0 \rightarrow a_1^-$ and $D^0 \rightarrow b_1^-$ transitions on q^2 are plotted in Fig. 4. In these plots, the LCSR results and the fitted form factors are displaced with circles and black lines, respectively. Moreover, the shaded regions are obtained using upper and lower values of the input parameters.

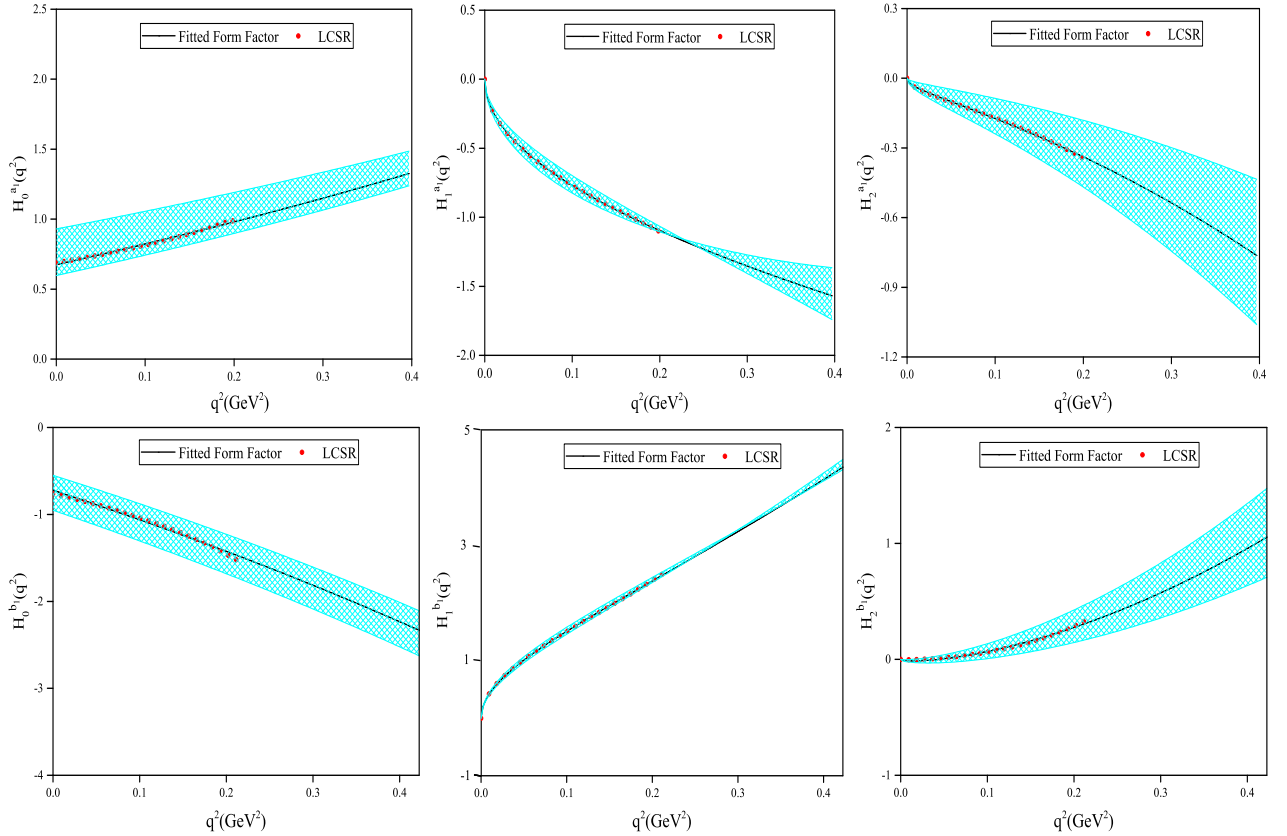


FIG. 4: $D^0 \rightarrow a_1^-$ and $D^0 \rightarrow b_1^-$ helicity form factors as a function of q^2 . Circles show the results of the LCSR while, black lines show the fitted form factors in the whole physical regions. The shaded bands stand for the results correspond the upper and lower values of the input parameters.

B. Analysis of the branching ratios

Now, we are ready to estimate the branching ratio values for the semileptonic $D_{(s)} \rightarrow A\ell\nu$ decays. The differential decay width of considered semileptonic decays is evaluated in SM as:

$$\frac{d\Gamma(D_{(s)} \rightarrow A\ell\nu)}{dq^2} = \frac{\sqrt{\lambda} G_F^2 |V_{cq'}|^2}{192 \pi^3 m_{D_{(s)}}^3} \left\{ [\mathcal{H}_0^A(q^2)]^2 + [\mathcal{H}_1^A(q^2)]^2 + [\mathcal{H}_2^A(q^2)]^2 \right\}, \quad (34)$$

where $V_{cq'} = V_{cd}(V_{cs})$ is used for $c \rightarrow d(s) \ell\nu$ transition. To calculate the branching ratios, the total mean life time $\tau_{D^0} = 0.41$, $\tau_{D^+} = 1.04$ and $\tau_{D_s^+} = 0.50$ ps [24] are used for the $D_{(s)}$ states. The differential branching ratios of $D^0 \rightarrow a_1^-(b_1^-)\ell\nu$ with their uncertainly regions, are plotted with respect to q^2 in Fig. 5. Moreover, our results for the branching ratio values of the semileptonic decays $D^0 \rightarrow a_1^-(b_1^-)\ell\nu$ and $D^+ \rightarrow a_1^0(b_1^0)\ell\nu$ decays as well as the estimations of the other approaches are presented in Fig. 6. The predictions of LCSR, 3PSR and CLFQM are calculated by using transition form factors.

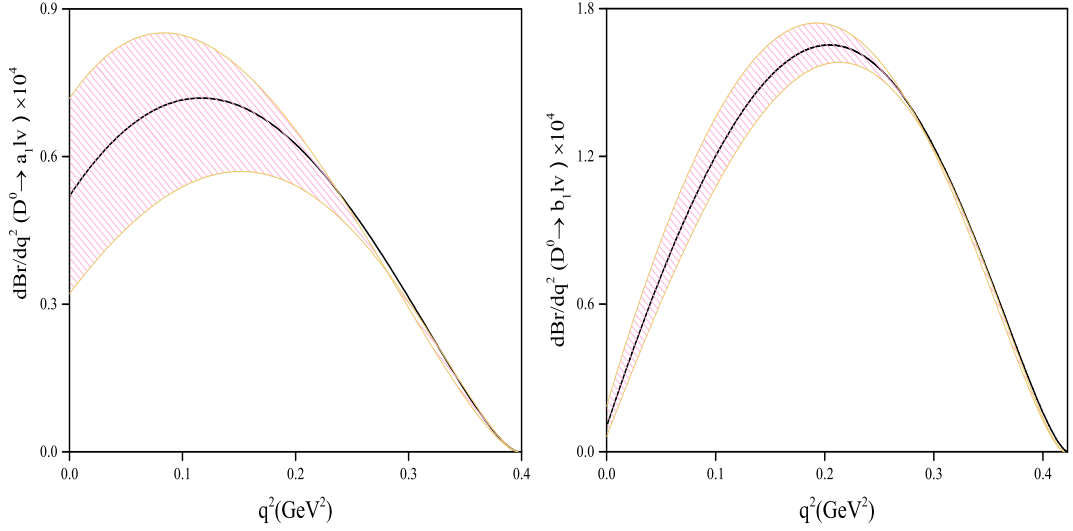


FIG. 5: The differential branching ratio of $D^0 \rightarrow a_1^-$ and $D^0 \rightarrow b_1^-$ decays as a function of q^2 . The shaded intervals show the results obtained using the upper and lower values of the input parameters.

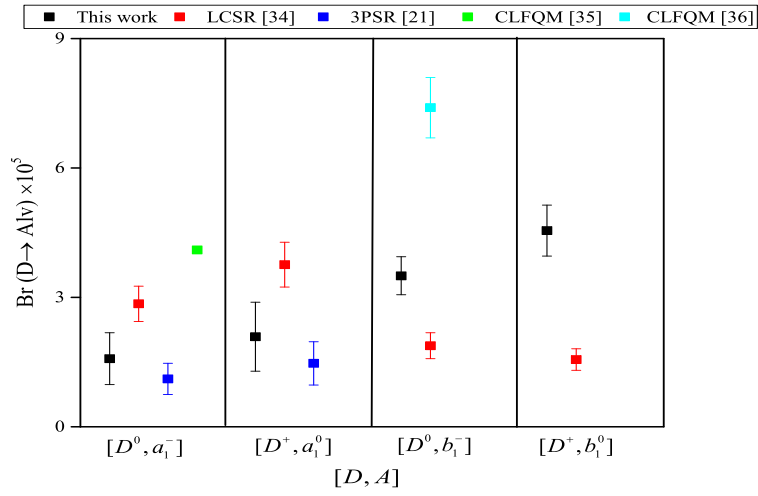


FIG. 6: Our predictions for branching ratio values of the semileptonic $D^0 \rightarrow a_1^-(b_1^-)\ell\nu$ and $D^+ \rightarrow a_1^0(b_1^0)\ell\nu$ decays. The results of the other methods, estimated using transition form factors, such as LCSR, 3PSR and CLFQM are also reported.

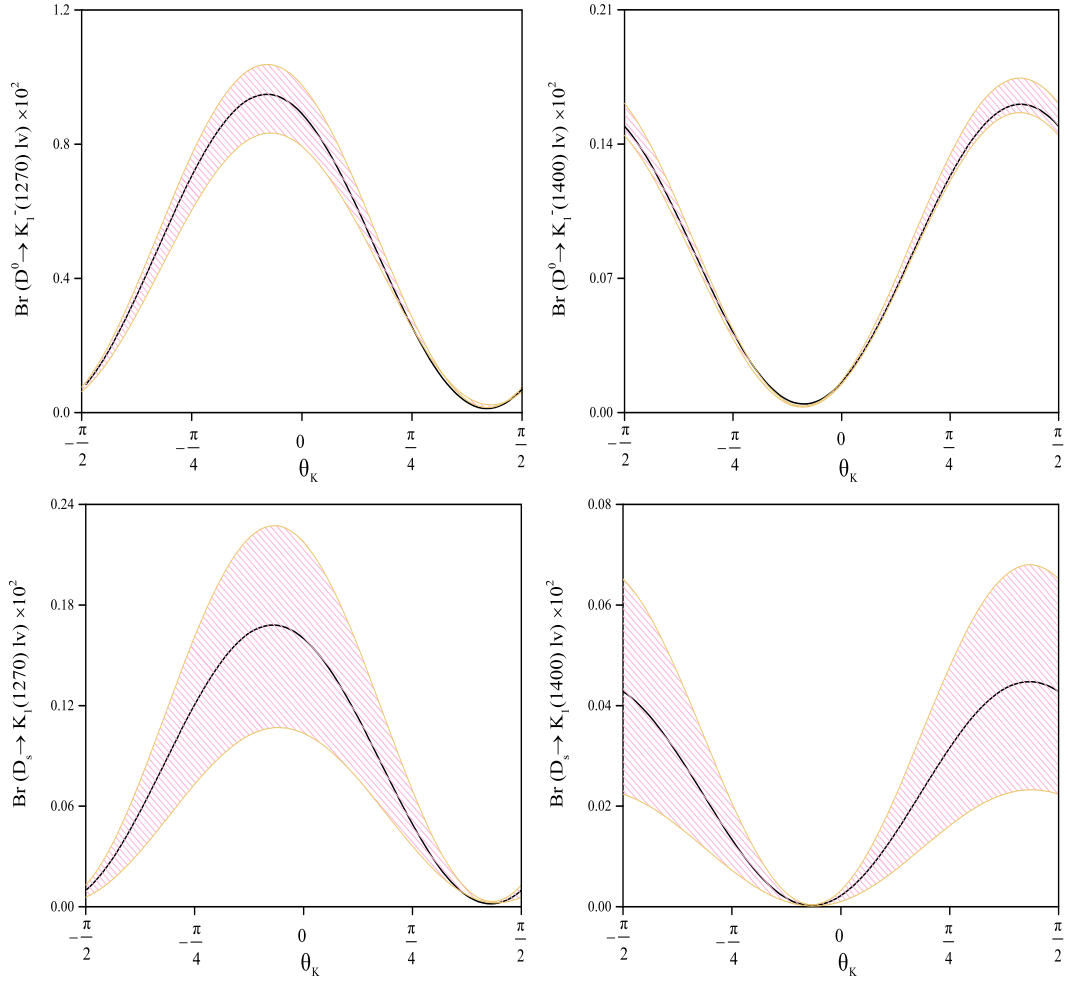


FIG. 7: The θ_K dependence of differential branching ratios of the semileptonic $D_{(s)} \rightarrow K_1(1270)\ell\nu$ and $D_{(s)} \rightarrow K_1(1400)\ell\nu$ transitions with their uncertainty bands.

The θ_K dependence of the branching ratio values of $D_{(s)}$ decays into the physical states $K_1(1270)$ and $K_1(1400)$, are displayed in Fig. 7; and comparison between our results and other theoretical techniques at $\theta_K = -(34 \pm 13)^\circ$ are given in Fig. 8. The $D^+ \rightarrow K_1^0(1270) e^+ \nu_e$ decay is searched at the BEPCII collider and its decay branching fraction is determined to be $\mathcal{B}(D^+ \rightarrow K_1^0(1270) e^+ \nu_e) = (2.30 \pm 0.69)$ [37]. Our branching ratio of $D^+ \rightarrow K_1^0(1270) e^+ \nu_e$ agrees with the experimental measurement when $\theta_K = -(36.68 \pm 6.30)^\circ$.

In summary, we calculate the $D_{(s)}$ to axial vector mesons $a_1^-, a_1^0, b_1^-, b_1^0, K_1(1270)$ and $K_1(1400)$ helicity form factors using the light cone QCD sum rules. The uncertainties of the helicity form factors come from the borel parameter M^2 , the charm quark mass m_c and Φ_\perp twist-2 light cone distribution amplitude of the axial vector meson. To extend the LCSR calculations to the full physical region, the extrapolated series expansions are used and the low-lying D meson resonances with 1^+ and 1^- quantum numbers were utilized as the dominant poles. Based on the fitted form factors, predictions for the branching ratios of relevant semileptonic decays were reported and a comparison was made between our results and other method estimations. Our calculation for branching ratio of $D^+ \rightarrow K_1^0(1270) e^+ \nu_e$ decay is in good agreement with the BEPCII collider measurement within errors at the mixing angle $\theta_K = -(36.68 \pm 6.30)^\circ$.

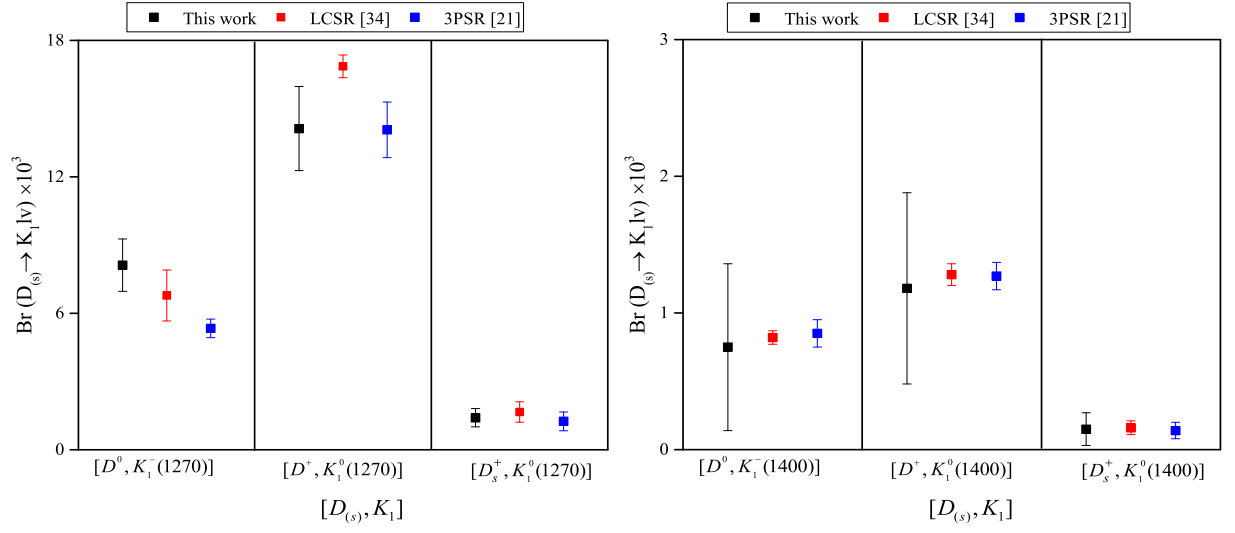


FIG. 8: Theoretical values for the branching ratio of the semileptonic $D_{(s)} \rightarrow K_1$ with $K_1 = K_1(1270), K_1(1400)$ at $\theta_K = -(34 \pm 13)^\circ$.

Appendix: Twist Function Definitions

In this appendix, we present the definitions for the two-parton LCDAs as well as the twist functions. Two-particle chiral-even distribution amplitudes are given by [31]:

$$\begin{aligned}
\langle 0 | \bar{q}_\alpha(x) q_\delta(0) | A(p, \varepsilon) \rangle &= -\frac{i}{4} \int_0^1 du e^{-iup' \cdot x} \left\{ f_A m_A \left[\not{p} \gamma_5 \frac{\varepsilon \cdot x}{p \cdot x} \Phi_{\parallel}(u) + \left(\not{\varepsilon} - \not{p} \frac{\varepsilon \cdot x}{p \cdot x} \right) \gamma_5 g_{\perp}^{(a)}(u) \right. \right. \\
&\quad \left. \left. - \not{x} \gamma_5 \frac{\varepsilon \cdot x}{2(p \cdot x)^2} m_A^2 \phi_b(u) + \epsilon_{\mu\nu\rho\sigma} \varepsilon^\nu p^\rho x^\sigma \gamma^\mu \frac{g_{\perp}^{(v)}(u)}{4} \right] \right. \\
&\quad \left. + f_A^\perp \left[\frac{1}{2} (\not{p} \not{\varepsilon} - \not{\varepsilon} \not{p}) \gamma_5 \Phi_{\perp}(u) - \frac{1}{2} (\not{p} \not{x} - \not{x} \not{p}) \gamma_5 \frac{\varepsilon \cdot x}{(p \cdot x)^2} m_A^2 \bar{h}_{\parallel}^{(t)}(u) \right. \right. \\
&\quad \left. \left. + i(\varepsilon \cdot x) m_A^2 \gamma_5 \frac{h_{\parallel}^{(p)}(u)}{2} \right] \right\}_{\delta\alpha}, \tag{35}
\end{aligned}$$

$$\begin{aligned}
\langle 0 | \bar{q}(x) \gamma_\mu \gamma_5 q'(0) | A(p, \varepsilon) \rangle &= i f_A m_A \int_0^1 du e^{-iup \cdot x} \left\{ p_\mu \frac{\varepsilon \cdot x}{p \cdot x} \Phi_{\parallel}(u) + \left(\varepsilon_\mu - p_\mu \frac{\varepsilon \cdot x}{p \cdot x} \right) g_{\perp}^{(a)}(u) + \mathcal{O}(x^2) \right\}, \\
\langle 0 | \bar{q}(x) \gamma_\mu q'(0) | A(p, \varepsilon) \rangle &= -i f_A m_A \epsilon_{\mu\nu\rho\sigma} \varepsilon^\nu p^\rho x^\sigma \int_0^1 du e^{-iup \cdot x} \left\{ \frac{g_{\perp}^{(v)}(u)}{4} + \mathcal{O}(x^2) \right\}, \tag{36}
\end{aligned}$$

also, two-particle chiral-odd distribution amplitudes are defined by:

$$\begin{aligned}
\langle 0 | \bar{q}(x) \sigma_{\mu\nu} \gamma_5 q'(0) | A(p, \varepsilon) \rangle &= f_A^\perp \int_0^1 du e^{-iup' \cdot x} \left\{ (\varepsilon_\mu p_\nu - \varepsilon_\nu p_\mu) \Phi_{\perp}(u) + \frac{m_A^2 \varepsilon \cdot x}{(p \cdot x)^2} (p_\mu x_\nu - p_\nu x_\mu) \bar{h}_{\parallel}^{(t)} + \mathcal{O}(x^2) \right\}, \\
\langle 0 | \bar{q}(x) \gamma_5 q'(0) | A(p, \varepsilon) \rangle &= f_A^\perp m_A^2 (\varepsilon \cdot x) \int_0^1 du e^{-iup \cdot x} \left\{ \frac{h_{\parallel}^{(p)}(u)}{2} + \mathcal{O}(x^2) \right\}. \tag{37}
\end{aligned}$$

In these expressions, f_A and f_A^\perp are decay constants of the axial vector meson A . We set $f_A^\perp = f_A$ in $\mu = 1$ GeV, such that we have

$$\langle 0 | \bar{q}(0) \sigma_{\mu\nu} \gamma_5 q'(0) | A(p, \varepsilon) \rangle = a_0^A f_A (\epsilon_\mu p_\nu - \epsilon_\nu p_\mu), \tag{38}$$

where a_0^\perp refers to the zeroth Gegenbauer moments of Φ_{\perp} . It should be noted that f_A is scale-independent and conserves G -parity, but f_A^\perp is scale-dependent and violates G -parity.

We take into account the approximate forms of twist-2 distributions for the $A = a_1, K_{1A}$ states to be [26]

$$\Phi_{\parallel}(u) = 6u\bar{u} \left[1 + 3a_1^{\parallel} \xi + a_2^{\parallel} \frac{3}{2} (5\xi^2 - 1) \right], \tag{39}$$

$$\Phi_{\perp}(u) = 6u\bar{u} \left[a_0^\perp + 3a_1^\perp \xi + a_2^\perp \frac{3}{2} (5\xi^2 - 1) \right], \tag{40}$$

and for the $A = b_1, K_{1B}$ to be

$$\Phi_{\parallel}(u) = 6u\bar{u} \left[a_0^{\parallel} + 3a_1^{\parallel} \xi + a_2^{\parallel} \frac{3}{2} (5\xi^2 - 1) \right], \tag{41}$$

$$\Phi_{\perp}(u) = 6u\bar{u} \left[1 + 3a_1^\perp \xi + a_2^\perp \frac{3}{2} (5\xi^2 - 1) \right], \tag{42}$$

where $\xi = 2u - 1$.

For the relevant two-parton twist-3 chiral-even LCDAs, we take the approximate expressions up to conformal spin $9/2$ and $\mathcal{O}(m_s)$ [26]:

$$\begin{aligned}
g_{\perp}^{(a)}(u) = & \frac{3}{4}(1 + \xi^2) + \frac{3}{2} a_1^{\parallel} \xi^3 + \left(\frac{3}{7} a_2^{\parallel} + 5 \zeta_{3,A}^V \right) (3\xi^2 - 1) \\
& + \left(\frac{9}{112} a_2^{\parallel} + \frac{105}{16} \zeta_{3,A}^A - \frac{15}{64} \zeta_{3,A}^V \omega_A^V \right) (35\xi^4 - 30\xi^2 + 3) \\
& + 5 \left[\frac{21}{4} \zeta_{3,A}^V \sigma_A^V + \zeta_{3,A}^A \left(\lambda_A^A - \frac{3}{16} \sigma_A^A \right) \right] \xi (5\xi^2 - 3) \\
& - \frac{9}{2} \bar{a}_1^{\perp} \tilde{\delta}_+ \left(\frac{3}{2} + \frac{3}{2} \xi^2 + \ln u + \ln \bar{u} \right) - \frac{9}{2} \bar{a}_1^{\perp} \tilde{\delta}_- (3\xi + \ln \bar{u} - \ln u),
\end{aligned} \tag{43}$$

$$\begin{aligned}
g_{\perp}^{(v)}(u) = & 6u\bar{u} \left\{ 1 + \left(a_1^{\parallel} + \frac{20}{3} \zeta_{3,A}^A \lambda_A^A \right) \xi \right. \\
& + \left[\frac{1}{4} a_2^{\parallel} + \frac{5}{3} \zeta_{3,A}^V \left(1 - \frac{3}{16} \omega_A^V \right) + \frac{35}{4} \zeta_{3,A}^A \right] (5\xi^2 - 1) \\
& + \frac{35}{4} \left(\zeta_{3,A}^V \sigma_A^V - \frac{1}{28} \zeta_{3,A}^A \sigma_A^A \right) \xi (7\xi^2 - 3) \left. \vphantom{\frac{35}{4}} \right\} \\
& - 18 \bar{a}_1^{\perp} \tilde{\delta}_+ (3u\bar{u} + \bar{u} \ln \bar{u} + u \ln u) - 18 \bar{a}_1^{\perp} \tilde{\delta}_- (u\bar{u}\xi + \bar{u} \ln \bar{u} - u \ln u),
\end{aligned} \tag{44}$$

$$\begin{aligned}
h_{\parallel}^{(t)}(u) = & 3a_0^{\perp} \xi^2 + \frac{3}{2} a_1^{\perp} \xi (3\xi^2 - 1) + \frac{3}{2} \left[a_2^{\perp} \xi + \zeta_{3,A}^{\perp} \left(5 - \frac{\omega_A^{\perp}}{2} \right) \right] \xi (5\xi^2 - 3) \\
& + \frac{35}{4} \zeta_{3,A}^{\perp} \sigma_A^{\perp} (35\xi^4 - 30\xi^2 + 3) + 18\bar{a}_2^{\parallel} \left[\delta_+ \xi - \frac{5}{8} \delta_- (3\xi^2 - 1) \right] \\
& - \frac{3}{2} \left(\delta_+ \xi [2 + \ln(\bar{u}u)] + \delta_- [1 + \xi \ln(\bar{u}/u)] \right) (1 + 6\bar{a}_2^{\parallel}),
\end{aligned} \tag{45}$$

$$\begin{aligned}
h_{\parallel}^{(p)}(u) = & 6u\bar{u} \left\{ a_0^{\perp} + \left[a_1^{\perp} + 5\zeta_{3,A}^{\perp} \left(1 - \frac{1}{40} (7\xi^2 - 3) \omega_A^{\perp} \right) \right] \xi \right. \\
& + \left(\frac{1}{4} a_2^{\perp} + \frac{35}{6} \zeta_{3,A}^{\perp} \sigma_A^{\perp} \right) (5\xi^2 - 1) - 5\bar{a}_2^{\parallel} \left[\delta_+ \xi + \frac{3}{2} \delta_- (1 - \bar{u}u) \right] \left. \vphantom{\frac{35}{6}} \right\} \\
& - 3[\delta_+ (\bar{u} \ln \bar{u} - u \ln u) + \delta_- (u\bar{u} + \bar{u} \ln \bar{u} + u \ln u)] (1 + 6\bar{a}_2^{\parallel}),
\end{aligned} \tag{46}$$

for $A = a_1, K_{1A}$ states, and

$$\begin{aligned}
g_{\perp}^{(a)}(u) = & \frac{3}{4} a_0^{\parallel} (1 + \xi^2) + \frac{3}{2} a_1^{\parallel} \xi^3 + 5 \left[\frac{21}{4} \zeta_{3,A}^V + \zeta_{3,A}^A \left(1 - \frac{3}{16} \omega_A^A \right) \right] \xi (5\xi^2 - 3) \\
& + \frac{3}{16} a_2^{\parallel} (15\xi^4 - 6\xi^2 - 1) + 5 \zeta_{3,A}^V \lambda_A^V (3\xi^2 - 1) \\
& + \frac{105}{16} \left(\zeta_{3,A}^A \sigma_A^A - \frac{1}{28} \zeta_{3,A}^V \sigma_A^V \right) (35\xi^4 - 30\xi^2 + 3) \\
& - 15\bar{a}_2^{\perp} \left[\tilde{\delta}_+ \xi^3 + \frac{1}{2} \tilde{\delta}_- (3\xi^2 - 1) \right] \\
& - \frac{3}{2} \left[\tilde{\delta}_+ (2\xi + \ln \bar{u} - \ln u) + \tilde{\delta}_- (2 + \ln u + \ln \bar{u}) \right] (1 + 6\bar{a}_2^{\perp}),
\end{aligned} \tag{47}$$

$$\begin{aligned}
g_{\perp}^{(v)}(u) = & 6u\bar{u} \left\{ a_0^{\parallel} + a_1^{\parallel} \xi + \left[\frac{1}{4} a_2^{\parallel} + \frac{5}{3} \zeta_{3,A}^V \left(\lambda_A^V - \frac{3}{16} \sigma_A^V \right) + \frac{35}{4} \zeta_{3,A}^A \sigma_A^A \right] (5\xi^2 - 1) \right. \\
& + \frac{20}{3} \xi \left[\zeta_{3,A}^A + \frac{21}{16} \left(\zeta_{3,A}^V - \frac{1}{28} \zeta_{3,A}^A \omega_A^A \right) (7\xi^2 - 3) \right] \\
& \left. - 5 \bar{a}_2^{\perp} [2\tilde{\delta}_+ \xi + \tilde{\delta}_- (1 + \xi^2)] \right\} \\
& - 6 \left[\tilde{\delta}_+ (\bar{u} \ln \bar{u} - u \ln u) + \tilde{\delta}_- (2u\bar{u} + \bar{u} \ln \bar{u} + u \ln u) \right] (1 + 6\bar{a}_2^{\perp}), \tag{48}
\end{aligned}$$

$$\begin{aligned}
h_{\parallel}^{(t)}(u) = & 3\xi^2 + \frac{3}{2} a_1^{\perp} \xi (3\xi^2 - 1) + \left[\frac{3}{2} a_2^{\perp} \xi + \frac{15}{2} \zeta_{3,A}^{\perp} \left(\lambda_A^{\perp} - \frac{1}{10} \sigma_A^{\perp} \right) \right] \xi (5\xi^2 - 3) \\
& + \frac{35}{4} \zeta_{3,A}^{\perp} (35\xi^4 - 30\xi^2 + 3) \\
& + \frac{9}{2} \bar{a}_1^{\parallel} \xi \left[\delta_+ (\ln u - \ln \bar{u} - 3\xi) - \delta_- \left(\ln u + \ln \bar{u} + \frac{8}{3} \right) \right], \tag{49}
\end{aligned}$$

$$\begin{aligned}
h_{\parallel}^{(p)}(u) = & 6u\bar{u} \left\{ 1 + a_1^{\perp} \xi + \left(\frac{1}{4} a_2^{\perp} + \frac{35}{6} \zeta_{3,A}^{\perp} \right) (5\xi^2 - 1) \right. \\
& + 5 \zeta_{3,A}^{\perp} \left[\lambda_A^{\perp} - \frac{1}{40} (7\xi^3 - 3) \sigma_A^{\perp} \right] \xi \left. \right\} \\
& - 9 \bar{a}_1^{\parallel} \delta_+ (3u\bar{u} + \bar{u} \ln \bar{u} + u \ln u) - 9 \bar{a}_1^{\parallel} \delta_- \left(\frac{2}{3} \xi u\bar{u} + \bar{u} \ln \bar{u} - u \ln u \right), \tag{50}
\end{aligned}$$

for $A = b_1, K_{1B}$ states. where

$$\tilde{\delta}_{\pm} = \frac{f_A^{\perp}}{f_A} \frac{m_{q_2} \pm m_{q_1}}{m_A}, \quad \zeta_{3,A}^{V(A)} = \frac{f_{3A}^{V(A)}}{f_A m_A}. \tag{51}$$

-
- [1] M. Artuso, B. Meadows and A. A. Petrov, *Ann. Rev. Nucl. Part. Sci* **58**, 249 (2008).
 - [2] T. Feldmann, B. Mueller and D. Seidel, *JHEP* **1708**, 105 (2017).
 - [3] J. Zhang, C. X. Yue, C. H. Li, *Eur. Phys. J. C* **78**, 695 (2018).
 - [4] A. Khodjamirian, R. Ruckl, S. Weinzierl, C. Winhart, and O. I. Yakovlev, *Phys.Rev. D* **62**, 114002 (2000).
 - [5] P. Ball, *Phys. Lett. B* **641**, 50 (2006).
 - [6] H. B. Fu, X. Yang, R. Lu, L. Zeng, W. Cheng and X. G. Wu, arXiv:1808.06412 [hep-ph].
 - [7] N. R. Soni and J. N. Pandya, *Phys. Rev. D* **96**, 016017 (2017).
 - [8] N. R. Soni, M. A. Ivanov, J. G. Korner, J. N. Pandya, P. Santorelli and C. T. Tran, arXiv:1810.11907 [hep-ph].
 - [9] W. Y. Wang, Y. L. Wu, and M. Zhong, *Phys. Rev. D* **67**, 014024 (2003).
 - [10] A. Abada et al. (SPQcdR collaboration), *Nucl. Phys. Proc. Suppl.* **119**, 625 (2003).
 - [11] C. Aubin et al. (Fermilab Lattice), *Phys. Rev. Lett.* **94**, 011601 (2005).
 - [12] C. Bernard et al., *Phys. Rev. D* **80**, 034026 (2009).
 - [13] I. Bediaga and M. Nielsen, *Phys. Rev. D* **68**, 036001 (2003).
 - [14] T. M. Aliev, V. L. Eletsky, and Ya. I. Kogan, *Sov. J. Nucl. Phys.* **40**, 527 (1984).
 - [15] P. Ball, V. M. Braun, and H. G. Dosch, *Phys. Rev. D* **44**, 3567 (1991).
 - [16] P. Ball, *Phys. Rev. D* **48**, 3190 (1993).
 - [17] A. A. Ovchinnikov and V. A. Slobodenyuk, *Z. Phys. C* **44**, 433 (1989); V. N. Baier and A. Grozin, *Z. Phys. C* **47**, 669 (1990).
 - [18] D. S. Du, J. W. Li, and M. Z. Yang, *Eur. Phys. J. C* **37**, 137 (2004).
 - [19] M. Z. Yang, *Phys. Rev. D* **73**, 034027 (2006); **73**, 079901(E) (2006).
 - [20] R. Khosravi, K. Azizi and N. Ghahramany, *Phys. Rev. D* **79**, 036004 (2009).
 - [21] Y. Zuo et al, *Int. J. Mod. Phys. A* **31**, 1650116 (2016).
 - [22] A. Bharucha, T. Feldmann and M. Wick, *JHEP* **1009**, 090 (2010).
 - [23] W. A. Bardeen, E. J. Eichten, and C. T. Hill, *Phys. Rev. D* **68**, 054024 (2003).
 - [24] C. Patrignani et al. (Particle Data Group), *Chin. Phys. C* **40**, 100001 (2016).
 - [25] W. Cheng, X. G. Wu, R. Y. Zhou and H. B. Fu, *Phys. Rev. D* **98**, 096013 (2018).
 - [26] K. Yang, *Nucl. Phys. B* **776**, 187 (2007).
 - [27] L. Burakovsky and T. Goldman, *Phys. Rev. D* **57**, 2879 (1998).
 - [28] M. Suzuki, *Phys. Rev. D* **47**, 1252 (1993).
 - [29] H. Y. Cheng, *Phys. Rev. D* **67**, 094007 (2003).
 - [30] H. Hatanaka, K. C. Yang, *Phys. Rev. D* **77**, 094023 (2008).
 - [31] K. Yang, *Phys. Rev. D* **78**, 034018 (2008).
 - [32] H. Mutuk, *Adv. Energy Phys.* **2018**, 8095653 (2018).
 - [33] M. C. Arnesen, B. Grinstein, I. Z. Rothstein, and I. W. Stewart, *Phys. Rev. Lett.*, **95**, 071802 (2005).
 - [34] S. Momeni and R. Khosravi, *J. Phys. G* **46**, 105006 (2019).
 - [35] W. Wang and Z. X. Zhao, *Eur. Phys. J. C* **76**, 59 (2016).
 - [36] H. Y. Cheng and X. W. Kang, *Eur. Phys. J. C* **77**, 369 (2017); *Eur. Phys. J. C* **77**, 863 (E) (2017).
 - [37] M. Ablikim et al. [BESIII Collaboration], arXiv: 1907.11370 [hep-ex].